

Molecular dynamics simulation of inertial trapping-induced atomic scale mass transport inside single walled carbon nanotubes

Z. L. Hu,^{1,2} Gustaf Mårtensson,¹ Murali Murugesan,¹ Xingming Guo,² and Johan Liu^{1,3,a)}

¹Chalmers University of Technology, Kemivägen 9, Se 412 96 Göteborg, Sweden

²Shanghai Institute of Applied Mathematics and Mechanics, Shanghai University, Yan Chang Road 149, Shanghai 200072, People's Republic of China

³Key Laboratory of New Displays and System Integration, SMIT Center and School of Mechatronics and Mechanical Engineering, Shanghai University, No 149, Yan Chang Road, Shanghai 200072, People's Republic of China

(Received 5 November 2012; accepted 11 February 2013; published online 28 February 2013)

The forced transverse vibration of a single-walled carbon nanotube (SWNT) embedded with atomic-size particles was investigated using molecular dynamic simulations. The particles inside the cylindrical cantilever can be trapped near the antinodes or at the vicinity of the SWNT tip. The trapping phenomenon is highly sensitive to the external driving frequencies such that even very small changes in driving frequency can have a strong influence on the probability of the location of the particle inside the SWNT. The trapping effect could potentially be employed to realize the atomic scale control of particle position inside an SWNT via the finite adjustment of the external driving frequency. It may also be suggested that the trapping phenomenon could be utilized to develop high-sensitive mass detectors based on a SWNT resonator. © 2013 American Institute of Physics. [<http://dx.doi.org/10.1063/1.4793533>]

Carbon nanotubes (CNT) provide a promising candidate toward the realization of the concepts concerning the manipulation of material at the nanoscale put forward by Feynman more than fifty years ago¹ because of their impressive geometrical, electrical, and mechanical properties. There are a number of different approaches that may be used to realize nanoscale mass transport^{2–15} based on CNT nanoelectromechanical systems (NEMS). The experimental approaches include electrophoretic,^{2–6} thermophoretic,^{7–9} and mechanically actuated^{10–15} methods. Electrophoretic methods can cause the motion of metal clusters^{2–5} or bio-molecules⁶ controlled by an external electric field. Phonon-assisted motion^{7,8} or thermal gradient⁹ mechanisms are reported as examples of thermophoretic methods of mass transport inside a CNT. As for mechanically assisted mass transport inside a CNT, various mechanisms have been put forward. Chang *et al.*¹⁰ proposed a mechanism to shoot out a C₆₀ molecule by stimulating a domino wave on a thick single-walled carbon nanotube (SWNT). Hu *et al.*¹¹ and Kan *et al.*¹² performed molecular dynamic simulations (MDS) of the transport of atomic mass driven by the bending of a CNT. Chen *et al.*¹³ and Qiu *et al.*¹⁴ further demonstrated that an excited vibrating CNT cantilever can act as an efficient and simple nanopump.

The above cases outlined the transportation of mass from one end of a CNT to the other, but few have attempted to do so in a controllable manner.^{3,6} Those works are thus still far from the goals of molecular manipulation envisioned by Feynman. Nevertheless, the study of the interaction of CNTs with nanoparticles caused by thermal excitations or mechanical vibrations^{15–21} is of fundamental and applied interest in the field of nanotechnology. Unfortunately, little

attention has been paid to CNT-based NEMS in nanoscale mass transport and manipulation using vibrations.^{4,13–15}

This paper addresses the specific problem of transporting atoms to a certain part of a CNT with the help of a resonance mechanism which offers a new route to mechanically assisted mass transport inside CNT via numerical MDS. The effect of external excited transverse mode vibrations on the motion of the monatomic molecules inside the SWNT-based NEMS cantilevers is studied. Due to inertial forces (centrifugal forces²⁰), the particles in a vibrating CNT have a tendency to move toward the antinodes and stay in the vicinity. The effects of “inertial trapping” for nanoparticles have been reported earlier in fluidic NEMS systems.²⁰ However, in the cited work, the “trapped” particles considered are of nanometer size. The analysis of the mass transport at that scale can be performed without the knowledge of the atom-atom confining potential. For the atomic-size particles, the non-uniform confining potential of the cantilever may cause a local “trapping” effect, or it may affect the dynamics in some other way. In particular, continuum models disregard the influence of thermal fluctuations, as well as strong non-linear effects in the van der Waals (vdW)-interaction between the tube and the particles. Therefore, MDS were employed to take all these factors into account.

The molecular model for the performed simulations is shown in Figure 1(a). The model is composed primarily of an SWNT-based NEMS cantilever that can be described by the continuum model (see Section A in supplementary material²³). The SWNT were placed in a Berendsen thermostat at a stable temperature of 30 K. The time step for the simulations was taken to be 0.5 fs, while the elapsed time in a typical simulation case is 5 ns. Other details of the simulations are provided in Section B in supplementary material.²³

Before the simulations of “inertial trapping,” the eigenfrequencies or the resonant frequencies of the SWNT system

^{a)}Author to whom correspondence should be addressed. Electronic mail: jliu@chalmers.se.

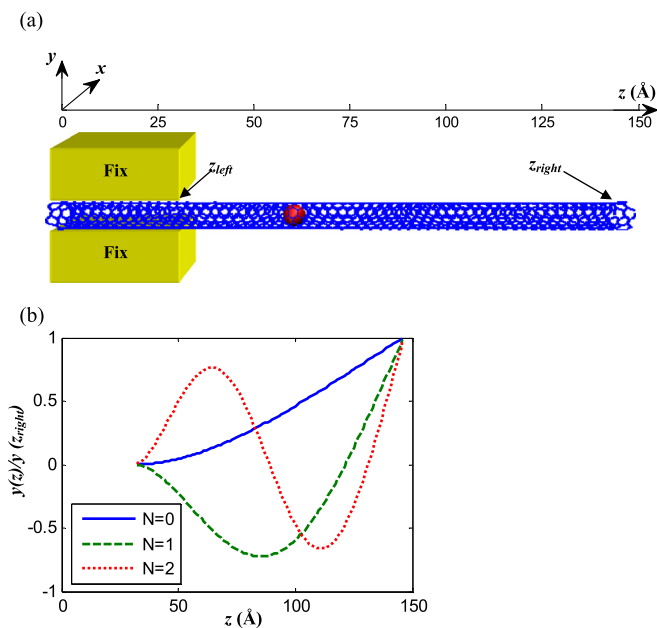


FIG. 1. The model for the “inertial trapping” simulations. (a) A schematic representation of the initial configuration. A 60 ring (5,5) SWNT was used. The inner particle (in red) was placed along the central axis of the SWNT (in blue). The left end of the SWNT axis acts as the origin of the coordinate system. The overall structure acts as a cantilever with $z \in [z_{left}, z_{right}]$, and a fixed prolongation with $z \in [0, z_{left}]$, where $z_{left} = 31 \text{ \AA}$ and $z_{right} = 144 \text{ \AA}$. Additionally, 50 carbon atoms near the position z_{left} were assigned as wiggling atoms and used to generate vibrations. (b) Normalized fundamental mode shapes for the first, second, and third transverse mode ($N = 0, 1, 2$) calculated in Section A in supplementary material.²³ The $N = 2$ mode is excited in the simulations.

were calculated (see Section C in supplementary material²³). Generally, it was found that when one or more particles are added to the cantilever, the eigenfrequencies of the system are changed with respect to the location of the particles, the mass and number of the particles, the amplitude of the vibrations, temperature, and the mode of vibration.

In order to check the phenomenon of “inertial trapping,” a particle was placed near the antinodes or the tip of the cantilever. The trajectories of the particle would then be analyzed to probe if the particle inside the cantilever would travel to and remain trapped near the antinodes or the SWNT tip, as well as remain there during the duration of the simulation. In this study, a krypton (Kr) atom was chosen as the particle, and the third transverse mode ($N = 2$) was excited, and thus two antinodes were formed (see Figure 1(b)). For this mode, the z -coordinates of the left and right antinodes are calculated to be approximately 60 \AA and 108 \AA , respectively. The chosen initial values for the z -coordinates of the particle were 60 \AA and 102 \AA . In the case of “inertial trapping” near the tip of the SWNT, the initial z -coordinate of the particle was chosen to be 130 \AA . According to calculations, if the particle stays near the left antinode, the right antinode, and the tip of the SWNT, the eigenfrequencies of the cantilever will be 334.5 GHz , 336.7 GHz , and 336.7 GHz , respectively. These frequencies were therefore used to excite the resonance vibrations in the simulations. More information concerning the simulations can be found in Section C in supplementary material.²³

The results from simulations utilizing resonance excitation are examined in this part. The resulting trajectories of

the particle in the SWNT in the z -direction are plotted in Figure 2(a). The green, red, and blue curves in Figure 2(a) show “inertial trapping” of the particle near the left antinode, the right antinode, and the tip of the cantilever, respectively. Related data are shown in Table I. While the particles are rotating in the xy -plane, as shown in Figure 2(c), the averaged z -coordinate of the particles are very close to the positions of antinodes or the tip, as shown in Table I. This can happen even if the initial z -coordinate of the particle is up to 6 \AA away from the antinode (see the red curve in Figure 2(a)). These results testify to the “inertial trapping” phenomenon for the third mode ($N = 2$) with one Kr particle inside the SWNT, within the simulation time span of 5 ns.

In Section D of the supplementary material,²³ details are given concerning alternative scenarios that test the trapping effect with different masses of particles, wiggling amplitudes, temperatures, etc.

After testing driving frequencies other than the eigenfrequency, we found that the trapping phenomenon is highly sensitive to the driving frequency. Cases where the Kr particle starts to move in the vicinity of the left antinode with $N = 2$ were simulated. The variance of the z -coordinate of the particle, V_z , is plotted in Figure 3 as a function of the driving frequency f . The results show that a small shift of less than 1% of f from the resonance frequency of 334.5 GHz can cause a considerable increase of V_z and a decrease of the quality of “inertial trapping.” Further analysis of the effect of the driving frequency shows that if f is smaller than 332.2 GHz or larger than 336.7 GHz , “inertial trapping” of the particle actually disappears totally. A similar trend was observed for cases where the particle starts to move from a position close to the right antinode with $N = 2$.

The inertia trapping phenomenon could potentially be applied to a number of applications. Two of these are presented hereafter. The first application that is put forth is the ability to control the position of a particle. The trapping phenomenon has been seen to be highly sensitive to the driving frequency of the CNT. It has also been found that the eigenfrequencies of the system are changed with respect to the location of the antinode close to which the particle resides (see Section B of supplementary material²³). The work presented in this paper suggests that the driving frequency could determine which antinode the particle will ultimately stably radiate to and thus control the position of the particle. An example of this manner of controlling has been demonstrated in the case, where the particle starts from a position near the right antinode, while the driving frequency $f = 334.5 \text{ GHz}$, which is the eigenfrequency for the particle at the left antinode. In this case, the particle could not remain near the right antinode and traveled to the left antinode after about 2 ns (see Figure 2(b) and associated video).

Another possible application of the “inertial trapping” phenomenon is to improve the sensitivity of CNT resonators for mass detection, an area of considerable recent interest. Jensen *et al.* reported the detection of a mass of $2/5 \text{ Au}$ atom, i.e., roughly a Kr-atom, utilizing a cantilever resonator.¹⁶ Chaste *et al.* declared that the mass of a proton can be detected by a double clamped resonator.¹⁷ The sensitivity can be expressed by the equivalent mass of the particle²² as

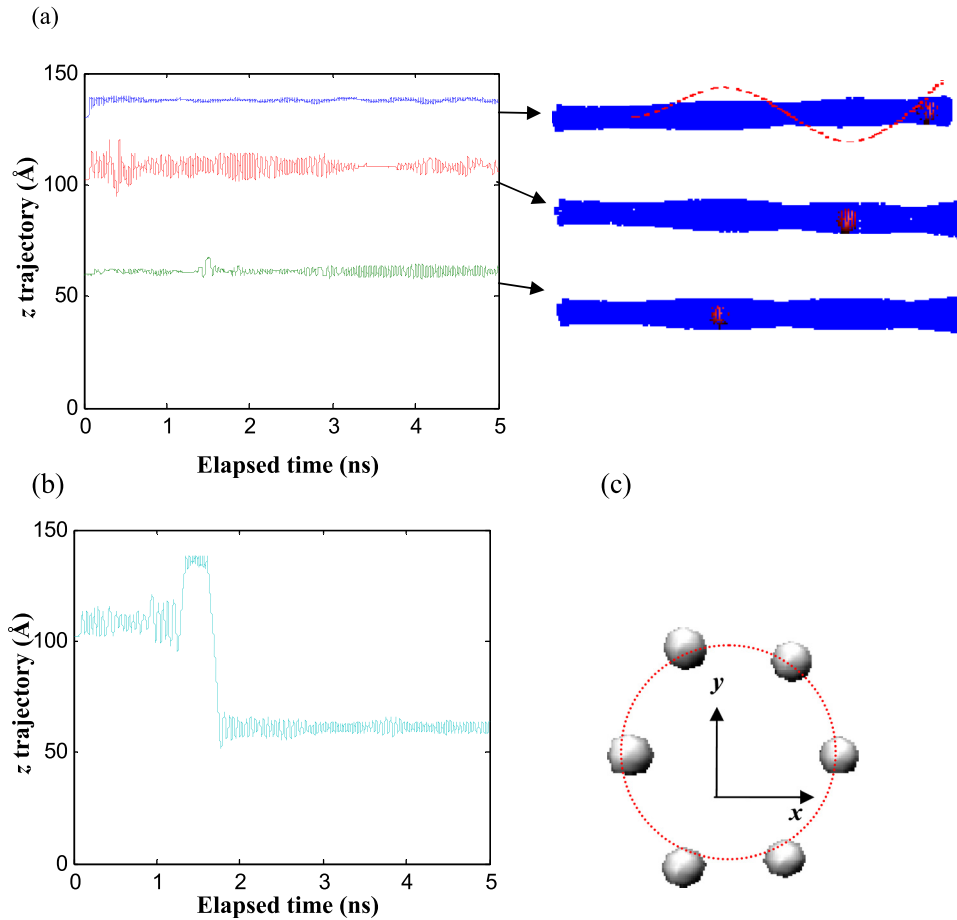


FIG. 2. Trajectory of the Kr particle in an SWNT. (a) The green, red, and blue curves show “inertia trapping” of the particle (in red color) with the third transverse vibration mode of the SWNT ($N=2$) depicted in blue near the left antinode, the right antinode, and the tip of the cantilever, respectively. The three subfigures on the right side are plotted by superimposing 20 frames separated by 25 ps intervals, where the mode shapes are shown; (b) an example of the breaking of “inertia trapping” with $N=2$. The particle was initially near the right antinode with a driving frequency of 334.5 GHz. (c) A plot of a trapped particle after superimposing 6 frames separated by 0.5 ps intervals, which shows a circular trajectory. The video demonstrates the controlling of the particle position as shown in (b) (enhanced online) [URL: <http://dx.doi.org/10.1063/1.4793533.1>].

$$m_r = m \int_{beam} p(z) \phi^2(z) dz, \quad (1)$$

where m is the mass of the particle, $p(z)$ is the probability that the particle will remain at z , and $\phi(z)$ is the profile of displacement of the axis of the SWNT. The equivalent mass m_r is proportional to the shift of the resonator’s resonance frequency. A larger m_r will therefore correspond to a higher sensitivity of the resonator. The best case scenario can be obtained when $m_r \approx m$ if the particle stays near the antinode, implying a small V_z . A high sensitivity is therefore obtained if a high degree of inertia trapping can be achieved.

TABLE I. The parameters that describe the “inertia trapping” phenomenon of the Kr particle inside the SWNT.

Antinode ^a	F (GHz) ^b	V_{yT} (Å ²) ^c	V_y (Å ²) ^c	V_z (Å ²) ^c	A_z (Å) ^d
Left	334.5	1.61	1.06	2.16	61.2
Right	336.7	1.24	0.58	7.52	108.2
Tip	336.7	1.27	0.47	0.40	137.8

^aThe antinode near which the particle is placed.

^bDriving frequencies. They are eigenfrequencies of the SWNT with $N=2$ and the Kr particle staying near the left antinode, the right antinode, and the tip of the cantilever, respectively.

^cThe variances of the y -coordinate at the apex of the SWNT cantilever, the y - and z -coordinates of the Kr particle. Here the V_z could be understood as the quality of the “inertia trapping.” Detailed physical meanings of these variances are in Section B in supplementary material.²³

^dThe averaged z -coordinate of the particle.

On the other hand, if the particle does not remain in a stable state in the vicinity of the antinode, m_r will be smaller. For example, the m_r can be estimated to be $0.27m$ for a cantilever at the third mode ($N=2$) with $p(z)=\text{constant}$. Considering that in reality that particle(s) can move in extended parts of the CNT, e.g., the fixed part in Figure 1(a) and that in experiments the extended parts are relatively long,¹⁸ m_r will be considerably smaller than m .

In conclusion, MDS have been employed for the analysis of the motion of an atomic size particle inside a vibrating SWNT. The forced transverse vibrations of a SWNT cantilever have been analyzed. It was found that the application of an external driving frequency to the system can lead to the

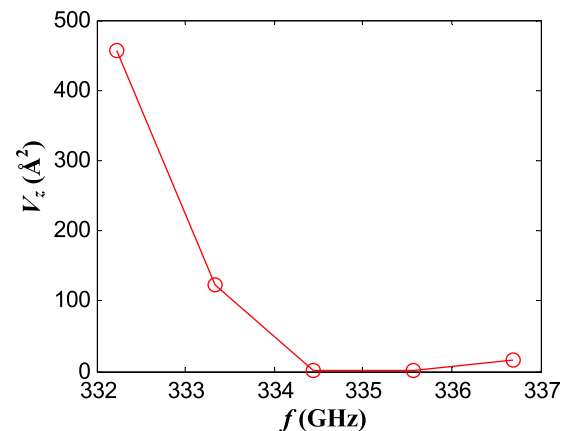


FIG. 3. Plot of the variance of the z -coordinate of the particle, V_z , as a function of the driving frequency f , which shows the sensitivity of the “inertia trapping” phenomenon to the driving frequency.

appearance of standing waves such that the particle will move inside the SWNT and be trapped either near the antinodes or in the vicinity of the SWNT tip. The particle's trapping phenomenon was found to be highly sensitive to the driving frequency such that a small change in the driving frequency will cause a large increase of variance of z -coordinate of the particle. The results suggest that it is possible to control the position of particle(s) by adjusting the SWNT driving frequency. It is also suggested that the trapping phenomenon can be utilized to improve the sensitivity of the CNT resonator for mass detection.

The authors acknowledge Juan Atalaya, Andreas Isacson, and Marina Voinova, Chalmers University of Technology for useful discussions and input concerning the innovation of the manuscript. The computations were performed on C3SE computing resources at Chalmers University of Technology. This work was supported in part by the Chinese Ministry of Science and Technology through the international collaboration program with the Contract No. 2010DFA14450, as well as by the EU programs Nanocom and Smartpower. This work was also carried out within the Sustainable Production Initiative and the Production Area of Advance at Chalmers University of Technology. This support is gratefully acknowledged. We also acknowledge the funding from the SSF Funding within the "Material for energy program" regarding thermo-electric materials (Contract No EMII-0002.006).

¹R. Feynman, *Caltech Eng. Sci.* **23**(5), 22 (1960), available at: <http://calteches.library.caltech.edu/1976/>.

- ²S. Regan, R. O. Aloni, U. D. Ritchie, and A. Zettl, *Nature (London)* **428**, 924–927 (2004).
- ³G. E. Begtrup, W. Gannett, T. D. Yuzvinsky, V. H. Crespi, and A. Zettl, *Nano Lett.* **9**, 1835–1838 (2009).
- ⁴K. Kim, K. Jensen, and A. Zettl, *Nano Lett.* **9**, 3209–3213 (2009).
- ⁵K. Svensson, H. Olin, and E. Olsson, *Phys. Rev. Lett.* **93**, 145901 (2004).
- ⁶P. Xiu, B. Zhou, W. Qi, H. Lu, Y. Tu, and H. Fang, *J. Am. Chem. Soc.* **131**, 2840–2845 (2009).
- ⁷P. A. E. Schoen, J. H. Walther, S. Arcidiacono, D. Poulidakos, and P. Koumoutsakos, *Nano Lett.* **6**, 1910–1917 (2006).
- ⁸P. A. E. Schoen, J. H. Walther, D. Poulidakos, and P. Koumoutsakos, *Appl. Phys. Lett.* **90**, 253116 (2007).
- ⁹B. R. Rurali, E. R. Hernández, J. Moser, T. Pichler, L. Forró, and A. Bachtold, *Science* **320**, 775–778 (2008).
- ¹⁰T. Chang, *Phys. Rev. Lett.* **101**, 175501 (2008).
- ¹¹Z. Hu, X. Guo, and J. Liu, *J. Comput. Theor. Nanosci.* **8**, 1716–1719 (2011).
- ¹²B. Kan, J. Ding, Z. Ling, N. Yuan, and G. Cheng, *Appl. Surf. Sci.* **256**, 3418–3422 (2010).
- ¹³M. Chen, J. Zang, D. Xiao, C. Zhang, and F. Liu, *Nano Res.* **2**, 938–944 (2009).
- ¹⁴H. Qiu, R. Shen, and W. Guo, *Nano Res.* **4**, 284–289 (2011).
- ¹⁵B. Li and T. Chang, *J. Appl. Phys.* **108**, 054304 (2010).
- ¹⁶K. Jensen, K. Kim, and A. Zettl, *Nat. Nanotechnol.* **3**, 533–537 (2008).
- ¹⁷J. Chaste, A. Eichler, J. Moser, G. Ceballos, R. Rurali, and A. Bachtold, *Nat. Nanotechnol.* **7**, 301 (2012).
- ¹⁸J. Chaste, M. Sledzinska, M. Zdrojek, J. Moser, and A. Bachtold, *Appl. Phys. Lett.* **99**, 213502 (2011).
- ¹⁹A. K. Huttel, G. A. Steele, B. Witkamp, M. Poot, L. P. Kouwenhoven, and H. S. J. van der Zant, *Nano Lett.* **9**, 2547–2552 (2009).
- ²⁰J. Lee, W. Shen, K. Payer, T. P. Burg, and S. R. Manalis, *Nano Lett.* **10**, 2537–2542 (2010).
- ²¹K. Jensen, J. Weldon, H. Garcia, and A. Zettl, *Nano Lett.* **7**, 3508 (2007).
- ²²L. D. Landau and E. M. Lifshitz, *Mechanics*, 3rd ed. (Elsevier, Amsterdam, 2004).
- ²³See supplementary material at <http://dx.doi.org/10.1063/1.4793533> for continuum analysis, details about MDS, calculation of the eigenfrequencies, and other simulated cases.